

# A theoretical comparison of multifunctional catalyst for sorption-enhanced reforming process



Elva L. Lugo, Benjamin A. Wilhite\*

Artie McFerrin Department of Chemical Engineering, Texas A&M University, 3122 TAMU, College Station, TX 77843-3122, United States

## HIGHLIGHTS

- Comparison of two one-pellet catalyst designs for sorption-enhanced processes.
- Both one-pellet designs had greater adsorbent utilization than a two-pellet design.
- Uniform-distributed design is recommended over core-shell due to better utilization.
- Core-shell design approaches uniform-distributed results at low catalyst thicknesses.
- Core-shell design mitigates hot-spot for an adiabatic sorption-enhanced WGS process.

## ARTICLE INFO

### Article history:

Received 4 September 2015

Received in revised form

4 April 2016

Accepted 5 April 2016

Available online 20 April 2016

### Keywords:

Sorption-enhanced reforming process

Multifunctional catalyst

CO<sub>2</sub> sequestration

Reaction-diffusion

Dusty-gas-model

## ABSTRACT

This work presents the first side-by-side comparison of the two leading multifunctional catalyst designs reported in the literature today for sorption-enhanced reforming processes. Two-dimensional unsteady-state models were developed to compare the performance of a core-shell multifunctional catalyst, consisting of a calcium-based sorbent core enclosed in a porous shell of methane steam reforming or water-gas shift catalyst, against an equivalent case of a uniform-distributed multifunctional design in which catalyst and sorbent materials are uniformly distributed within the particle. Additionally, these two multifunctional catalyst designs were compared against the conventional two-pellet approach, where the capture and catalytic properties are distinguished into separate pellets. Both multifunctional catalyst designs (i.e. core-shell and uniform-distributed) had greater adsorbent utilization and higher H<sub>2</sub> outlet concentration up to breakthrough time than the conventional two pellet design. The uniform-distributed multifunctional catalyst design had greater adsorbent utilization up to breakthrough conditions as compared to the core-shell design. This behavior may be attributed to the fact that for the uniform-distributed multifunctional, the active catalyst is constantly producing CO<sub>2</sub> next to an adsorbent active site. For the core-shell multifunctional catalyst design, decreasing catalyst-shell thickness resulted in performance approaching the uniform-distributed case. For the case of exothermic water-gas shift reaction coupled with CO<sub>2</sub> chemisorption, the core-shell design mitigated local bed hot-spot magnitudes by ~40 K.

© 2016 Elsevier Ltd. All rights reserved.

## 1. Introduction

Sorption-enhanced reforming processes (SERPs), in which catalytic reaction is directly coupled with CO<sub>2</sub> adsorption, have received significant attention over the past two decades owing to a growing demand for high-purity H<sub>2</sub> and rising costs associated with CO<sub>2</sub> by-product emissions (Barelli et al., 2008; Ochoa-Fernández et al., 2007). Methane steam reforming (MSR) and water-gas shift (WGS) (Eqs. (1) and (2), respectively) are two key

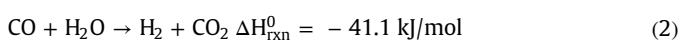
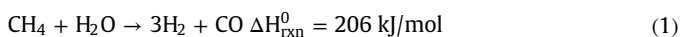
reactions in hydrogen production today (Holladay et al., 2009; Leiby, 1994). Both MSR and WGS are equilibrium-limited reactions and, therefore, require additional capital cost associated with multi-staged beds to maximize H<sub>2</sub> yield (Satterfield, 1991). The product reformat stream needs further purification to achieve H<sub>2</sub> purities > 95% as required by many of refinery operations (Alves and Towler, 2002; Harrison, 2008; Zagoria and Huyck, 2003). Purification processes based upon the selective removal of H<sub>2</sub> from the reformat stream result in rejection losses which translate to H<sub>2</sub> waste, and do not offer a direct means to capture CO<sub>2</sub> for appropriate utilization or disposal. Process intensification via SERP addresses these challenges by isolating CO<sub>2</sub> from the reacting fluid, thereby removing equilibrium limitation on hydrogen yield while

\* Corresponding author.

E-mail address: [benjaminwilhite@mail.che.tamu.edu](mailto:benjaminwilhite@mail.che.tamu.edu) (B.A. Wilhite).

Nomenclature		Z	molar volume ratio, $V_{\text{CaCO}_3}/V_{\text{CaO}}$ , dimensionless
$B_0$	permeability coefficient, $\text{m}^2$	<i>Greek symbols</i>	
$c_i$	concentration of component $i$ , $\text{mol m}^{-3}$	$\alpha$	adsorbent-to-catalyst volume ratio, dimensionless
$C_p$	specific heat capacity, $\text{J mol}^{-1} \text{K}^{-1}$	$\delta$	average grain diameter, m
$d$	particle diameter, m	$\Delta H_{\text{rxn}}^0$	heat of reaction, $\text{J mol}^{-1}$
$D_{ij}$	binary diffusion coefficient of a mixture $i$ and $j$ , $\text{m}^2 \text{s}^{-1}$	$\epsilon$	porosity, dimensionless
$D_{i,k}$	Knudsen diffusion coefficient of component $i$ , $\text{m}^2 \text{s}^{-1}$	$\epsilon/\kappa$	Lennard-Jones parameter, K
$D_{z,i}$	axial dispersion coefficient of component $i$ , $\text{m}^2 \text{s}^{-1}$	$\zeta$	defined in Eq. (45), dimensionless
$Da$	Damköhler number, dimensionless	$\eta$	effectiveness factor, dimensionless
$E_a$	activation energy, $\text{J mol}^{-1}$	$\Theta$	defined in Eq. (29), dimensionless
$F_{\text{press}}$	pressure scale-up factor, dimensionless	$\lambda_T$	axial bed conductivity, $\text{J m}^{-1} \text{s}^{-1} \text{K}^{-1}$
$k$	thermal conductivity, $\text{J m}^{-1} \text{s}^{-1} \text{K}^{-1}$	$\mu_i$	viscosity of component $i$ , Pa s
$k_f$	rate constant, $\text{mol m}^3 \text{s}^{-1}$	$v_i$	diffusion volume of component $i$ , dimensionless
$k_{gs}$	mass transfer coefficient at gas-solid interface, $\text{mol m}^{-2} \text{s}^{-1}$	$\Phi$	modified Thiele Modulus, dimensionless
$k_s$	kinetic constant for surface reaction, $\text{m}^4 \text{kmol}^{-1} \text{h}^{-1}$	$\rho$	density, $\text{m}^3 \text{kg}^{-1}$
$K_{\text{eq}}$	reaction equilibrium constant, dimensionless for WGS and (Pa) for MSR	$\sigma$	Lennard-Jones parameter, Å
$M_i$	molecular weight of species $i$ , $\text{kg mol}^{-1}$	$\sigma_{\text{CaO}}$	grain surface area per unit particle volume, $\text{m}^{-1}$
$N_{\text{Ca}}$	moles per unit volume of sorbent particle, $\text{kmol m}^{-3}$	$\tau$	tortuosity factor, dimensionless
$N_i$	flux of component $i$ , $\text{mol m}^{-2} \text{s}^{-1}$	$\Omega$	Lennard-Jones parameter, dimensionless
$Nu$	Nusselt number, dimensionless	<i>Subscripts</i>	
$p_i$	partial pressure of component $i$ , Pa	0	initial/inlet condition
$P$	pressure, Pa	b	bulk
$Q_r$	rate of heat generation, $\text{J mol}^{-1} \text{s}^{-1}$	CaO	calcium oxide
$r_i$	rate of appearance of component $i$ via WGS/MSR reaction, $\text{mol m}^{-3} \text{s}$	Cat	catalyst
$r_p$	pore radius, m	CO	carbon monoxide
$R_1$	sorbent radius of core-shell design, m	CO <sub>2</sub>	carbon dioxide
$R_2$	sorbent plus catalyst radius of core-shell design, m	MET	methanation
$Re$	Reynolds number, dimensionless	H <sub>2</sub>	hydrogen
$R_g$	universal gas constant, $\text{J mol}^{-1} \text{K}^{-1}$	H <sub>2</sub> O	steam
$Sc$	Schmidt number, dimensionless	mix	mixture
$Sh$	Sherwood number, dimensionless	MSR	methane steam reforming
$T$	temperature, K	p	pellet
$t$	time, s	sor	sorbent
$t_c$	catalyst-shell thickness, m	WGS	water gas shift
$u$	velocity, $\text{m s}^{-1}$	<i>Superscript</i>	
$V$	molar volume, $\text{m}^3 \text{mol}^{-1}$	eff	effective
$X$	local extent of solid sorbent conversion, dimensionless		
$x_i$	mole fraction of component $i$ , dimensionless		
$z$	axial coordinate, dimensionless		

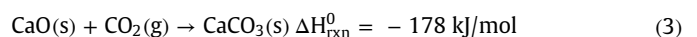
simultaneously purifying the product stream. Although SERPs eliminate the need for a separate purification stage, these processes generate an additional cost due to the need for adsorbent regeneration. The advantages of lower capital cost and reduced footprint resulting from the selection of the SERP technology must be weighed against the additional cost arising from the regeneration process in order to select the best approach.



The selected adsorbent must be capable of CO<sub>2</sub> adsorption at the conditions of the reactions (473–1023 K). CaO-based adsorbents are ideal candidates for SERP processes because they are inexpensive and abundant. However, the main disadvantage of adsorbents derived from natural sources is the decay of their capacity to capture CO<sub>2</sub> with each passing cycle as well as their poor mechanical stability (Anthony, 2008; Blamey et al., 2010; Grasa

and Abanades, 2006). These disadvantages can be mitigated by blending CaO with refractory materials (e.g., MgO, ZrO, CaTiO<sub>3</sub>) to prevent pore closure during the regeneration process and improve material's mechanical properties (Harrison, 2008).

Sorption of CO<sub>2</sub> occurs via the reversible exothermic reaction of CO<sub>2</sub> and CaO (Eq. 3) that yields to CaCO<sub>3</sub> in the solid phase (Abanades and Alvarez, 2003; Huijgen and Comans, 2003; Sten-dardo and Foscolo, 2009). Inspection of the equilibrium CO<sub>2</sub> pressure over CaO indicates that H<sub>2</sub> purification via CO<sub>2</sub> sorption using CaO-based adsorbents is compatible with MSR and WGS operating conditions (Harrison, 2008).



The majority of reports on sorption-enhanced methane steam reforming (SEMSR) and sorption-enhanced water-gas shift (SEWGS) have focused upon a two-pellet design, where the adsorptive and catalytic properties are distinguished into separate pellets (Jang et al., 2013; Jang et al., 2012; Stevens et al., 2010; Van

Download English Version:

<https://daneshyari.com/en/article/154358>

Download Persian Version:

<https://daneshyari.com/article/154358>

[Daneshyari.com](https://daneshyari.com)